

Isothermal Crystallization Kinetics in Binary Miscible Blend of Poly(ϵ -caprolactone)/Tetramethyl Polycarbonate

Samy A. Madbouly

Department of Chemistry, Faculty of Science, Cairo University, Orman, Giza 12613, Egypt

Received 2 June 2006; accepted 6 August 2006

DOI 10.1002/app.25834

Published online 27 October 2006 in Wiley InterScience (www.interscience.wiley.com).

ABSTRACT: The crystallization kinetics of pure poly(ϵ -caprolactone) (PCL) and its blends with bisphenol-A tetramethyl polycarbonate (TMPC) was investigated isothermally as a function of composition and crystallization temperature (T_c) using differential scanning calorimetric (DSC) and polarized optical microscope techniques. Only a single glass-transition temperature, T_g , was determined for each mixture indicating that this binary blend is miscible over the entire range of composition. The composition dependence of the T_g for this blend was well described by Gordon–Taylor equation with $k = 1.8$ (higher than unity) indicating strong intermolecular interaction between the two polymer components. The presence of a high T_g amorphous component (TMPC) had a strong influence on the crystallization kinetics of PCL in the blends. A substantial decrease in the crystallization kinetics was observed as the concentration of TMPC rose in the blends. The crystallization half-time $t_{0.5}$ increased monotonically with the crystal-

lization temperature for all composition. At any crystallization temperature (T_c) the $t_{0.5}$ of the blends are longer than the corresponding value for pure PCL. This behavior was attributed to the favorable thermodynamics interaction between PCL and TMPC which in turn led to a depression in the equilibrium melting point along with a simultaneous retardation in the crystallization of PC. The isothermal crystallization kinetics was analyzed on the basis of the Avrami equation. Linear behavior was held true for the augmentation of the radii of spherulites with time for all mixtures, regardless of the blend composition. However, the spherulites growth rate decreased exponentially with increasing the concentration of TMPC in the blends. © 2006 Wiley Periodicals, Inc. *J Appl Polym Sci* 103: 3307–3315, 2007

Key words: isothermal crystallization kinetics; Avrami approach; growth rate

INTRODUCTION

The crystallization behavior of blend containing at least one semicrystalline polymer component is not only of theoretical interest for understanding polymer morphology, but also of basic importance in practical operations such as in plastics fabrication as extrusion and spinning of molten polymers. The crystallization and melting behavior of crystalline polymers are often influenced by the presence of other components. It is well established that the structural parameters such as lamellar thickness, crystal interphase, and spherulitic growth rates are substantially modified by further components.^{1–3} Moreover, from the thermodynamic point of view, a depression in the equilibrium melting point would occur as a result of specific interaction between the two components of the blend and also because of changes in the free energy required in the formation of crystals. Determination of the interaction parameters between two polymer components is crucial to understand

the phase behavior and miscibility of the mixtures. Special attention has been paid to evaluate the interaction parameter from the melting point depression of crystalline polymer blends.

A huge number of literature studies for the influence of amorphous polymers on the crystallization behavior of crystalline polymers have been reported.^{4–13} Ullmann and Wendorff⁴ have shown that the lamellar thickness of poly(vinylidene fluoride) (PVDF) decreases with increasing the concentration of poly(methyl methacrylate) (PMMA) in the blend. The radial growth rate of poly(ethylene oxide) (PEO) spherulites decreases and its half-time of crystallization increases at a given crystallization temperature in the PEO/PMMA and PEO/poly(vinyl acetate) (PVAc) blends.⁵ Many authors have also reported the depression of the melting points for crystalline/amorphous polymer blends.^{6–11}

Poly(ϵ -caprolactone) (PCL) represents an important class of semicrystalline polymers as a potential replacement for conventional polymers because of its biodegradability, favorable miscibility with other polymers, and low-temperature adhesiveness.¹⁴ Numerous studies have been carried out for modifying PCL by blending or copolymerization with other polymers.^{15–24} The miscibility of PCL/poly(styrene-co-acrylonitrile) (SAN) blend and the influence of acrylonitrile

Correspondence to: S. A. Madbouly (Samy.Madbouly@usm.edu).

(AN) content in the copolymer upon blend miscibility have been studied by Chiu and Smith.²⁰ They found that SAN and PCL are miscible when the AN content in SAN ranges from 8 to 28 wt %. Savoboda et al.^{21,22} studied the morphology of PCL/SAN blend via competition with spinodal decomposition. The kinetics of spinodal decomposition was quantitatively evaluated using V_v light scattering technique. Vanneste and Groeninckx²³ investigated the miscibility and phase behavior of PCL/SAN/poly(styrene-*co*-maleic anhydride) (SMA) ternary blend by means of visual observation, light transmission, differential scanning calorimetry (DSC), and dynamic mechanical thermal analysis. The competition between crystallization and phase separation of PCL/PS blend has been investigated using small-angle X-ray scattering by Li and Jungnickel.²⁴

The isothermal crystallization kinetics can adequately be described by Avrami analysis, which remains the most popular method for obtaining information about bulk crystallization kinetics.^{25–27} The nonisothermal crystallization is rather complicated and can be described either by a modified Avrami analysis which considers the isothermal process as a sequence of infinitesimally small isothermal stages^{28–30} or by Ozawa analysis which uses the cooling rate instead of the crystallization time in the Avrami equation.^{31,32} All methods provide qualitative information about bulk crystallization kinetics and should be complemented by microscopic investigations.

The objective of the present work was to investigate the influence of a high T_g amorphous component (bisphenol-A tetramethyl polycarbonate (TMPC) with $T_g = 190^\circ\text{C}$) on the isothermal crystallization kinetics of PCL in the blends using DSC and polarized optical microscope. The crystallization kinetics will be investigated as a function of TMPC composition at different crystallization temperatures. The data will be analyzed on the basis of Avrami approach for the isothermal crystallization kinetics. In addition the Hoffman–Weeks plot will be employed to evaluate the equilibrium melting point for different blend compositions. Consequently, the thermodynamic interaction parameters will be obtained from the melting point depression based on Flory–Huggins approach. The crystal growth rates measured by polarized optical microscope as the radial growth rate of spherulites will be analyzed as a function of blend composition.

EXPERIMENTAL

Materials and sample preparation

The PCL used in this work was a commercial one of Union Carbide Corporation, USA (PCL-767; $M_w = 40,400$ g/mol, $M_w/M_n = 2.61$). TMPC was obtained

from Bayer, Leverkusen, Germany; the molecular weight (M_w) of TMPC is 40,000 g/mol.

The PCL and TMPC blends were prepared by dissolving the two polymer components in toluene. The blend solutions were then cast onto Petri dishes and left to dry at room temperature for about 3 days, and after that, complete drying of the blends until constant weight was accomplished under vacuum for another 3 days at 80°C .

Optical microscope

The spherulitic morphologies of PCL in the blends were observed with an Olympus BH-2 equipped with polarizer, a video recording system, and an exposure control unit (Olympus PM-20). The blends were melted at 100°C for 5 min to erase the previous thermal history and then were quickly quenched to the crystallization temperature ($T_c = 40^\circ\text{C}$).

Thermal analysis

The calorimetric measurements were carried out using a DSC Seiko Instrument EXSTAR 6000 in the atmosphere of dry nitrogen. The instrument was calibrated with In, Sn, and Pb standards. The calorimetric glass temperatures of the blends (T_{gs}) were determined at $10^\circ\text{C}/\text{min}$ heating rate. The T_g was defined as the temperature of the half of the step height in specific heat curves.

The isothermal crystallization process can be summarized by the following four experimental steps:

1. Rapid heating of the sample to the melting temperature, $T_m = 100^\circ\text{C}$ (T_m is higher than the upper limit of the melting endotherm).
2. Holding the molten sample at T_m for 5 min.
3. Rapid cooling at $70^\circ\text{C}/\text{min}$ from T_m to the crystallization temperature (T_c).
4. Isothermal crystallization of the semicrystalline component in the blend at $T = T_c$.

The crystallization process was completed within 2–60 min according to the values of crystallization temperatures. The optimum crystallization temperature range for pure PCL and blends was $T_c = 35\text{--}45^\circ\text{C}$.

The melting points (T_m) for the blends that were completely crystallized at different T_c were also determined at $10^\circ\text{C}/\text{min}$ heating rate.

RESULTS AND DISCUSSION

Glass-transition temperature

The prepared samples of PCL/TMPC were optically clear, and no structure was observed under the

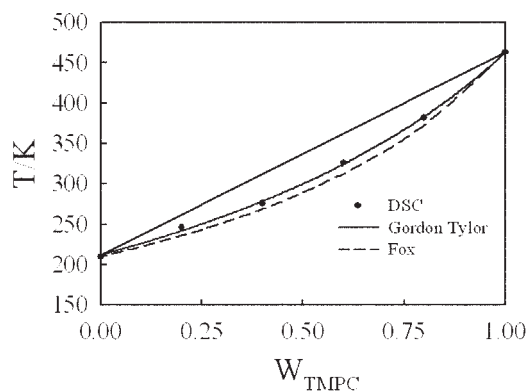


Figure 1 Calorimetric T_{gs} of the blends as a function of composition (●). The dashed line is the calculated line using Fox equation; while the solid line is the fitting line given by Gordon–Taylor equation.

microscope even at very high temperatures ($T \leq 280^\circ\text{C}$) above the melting temperature of PCL. The calorimetric glass-transition temperatures T_{gs} of the blends determined by DSC as a function of composition are demonstrated in Figure 1. Only one common T_g was observed and its value was located between the T_{gs} of the pure components, i.e., the two components are miscible over the entire range of composition. A number of empirical models were proposed to predict the composition dependence of glass-transition temperatures in miscible polymer blends. The simple mixing rule, Fox and Gordon–Taylor equations are some of those empirical models.^{33,34} This blend shows a negative deviation from the linear mixing rule as observed in some other polymer blends such as TMPC/PS³⁵ and P α MSAN/PMMA.³⁶ The composition dependence of T_g for this blend can not be given by Fox equation which is commonly used to describe the T_g versus ϕ in many polymer blends³³:

$$\frac{1}{T_g} = \frac{w_1}{T_{g1}} + \frac{w_2}{T_{g2}} \quad (1)$$

where w_i and T_{gi} are the weight fraction and glass-transition temperature of component i , respectively, while T_g is the glass-transition temperature of the blend. The line (dashed line in Fig. 1) calculated from the above equation is clearly deviated from the experimental data and somewhat locates at lower temperatures. This deviation from Fox equation may be attributed to the favorable interaction between the two polymer components which leads in turn to higher T_{gs} than that estimated by Fox equation. For this reason we checked Gordon–Taylor equation³⁴ to represent the composition dependence of T_g for this blend:

$$T_g = \frac{w_1 T_{g1} + k w_2 T_{g2}}{w_1 + k w_2} \quad (2)$$

with $k = \Delta C_{p2} / \Delta C_{p1}$, where ΔC_{p2} and ΔC_{p1} are the heat capacity change for pure PCL and TMPC, respectively. This equation was derived based on thermodynamic arguments for the entropy of mixing of two polymers, assuming temperature-independent heat capacity increments and also assuming that miscibility approached the segmental level. The value of k is correlated to the intensity of the interaction between the two polymer components. The solid line passes through the values of the T_{gs} in Figure 1 is the calculated line using the above equation with $k = 1.8$ (the best value obtained from the fitting). It is obvious that Gordon–Taylor equation (solid line) gives a better representation of the data than that given by Fox equation (dashed line). The value of k is higher than unity, indicating that the two components are favorably interacted with each other. This favorable interaction is the direct reason for the negative deviation of T_g versus composition from the simple mixing rule. This behavior suggests that when the intimate mixing takes place, PCL molecules are more mobile than TMPC because of the very low T_g of PCL compared with that of TMPC (Fig. 1). The molecules of PCL component are then driven by this interaction force to surround the TMPC monomer units. The presence of a high number of PCL monomer units neighboring TMPC monomer units as compared with simple mixing rule would explain the observed negative deviation of T_g versus composition.

Equilibrium melting point and interaction parameter

The depression in the melting point of crystalline component in amorphous/crystalline polymer blends can reveal important information about miscibility and polymer–polymer interaction parameters. This depression in the melting point can be related to morphological and thermodynamical effects. The morphological effect can be easily eliminated by using the equilibrium melting point instead of the melting point. Many authors use the Hoffman–Weeks³⁷ plot to obtain information on the equilibrium melting temperature T_m^0 from measurements of T_m for the sample that was crystallized at different constant temperatures, T_c . According to this procedure, the intersect of T_c versus T_m with the line defined by $T_c = T_m$ should yield T_m^0 . Typical Hoffman–Weeks plots for the pure PCL and different blend compositions are shown in Figure 2. Obviously the values of T_m^0 are strongly influenced by composition, i.e., decrease with increasing the concentration of TMPC in the blend. The equilibrium melting points obtained by Hoffman–Weeks plots are shown as a function of composition in the inset-plot of Figure 2. The equilibrium melting point decreases linearly with increasing the concentration of amorphous component (TMPC) in the blend.

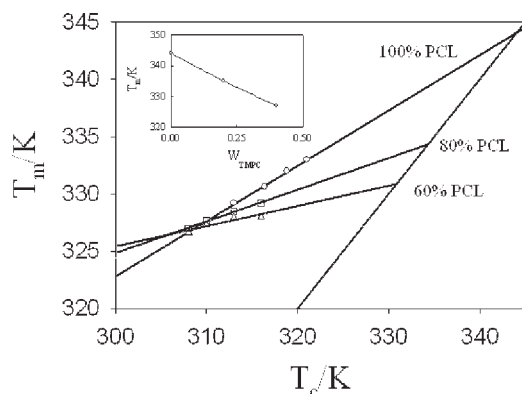


Figure 2 Hoffman-Weeks plots for PCL/TMPC blends. The inset-plot shows the composition dependence of equilibrium melting points T_m obtained by Hoffman-Weeks plots.

The melting point depression of the crystalline polymer component in blend depends on the strength of thermodynamic interaction between the two components. Generally, for immiscible or partially miscible polymer blends, there is no any depression in the equilibrium melting point of the crystalline polymer component. The depression in the equilibrium melting point is typically observed in miscible blends because of the favorable interaction between the crystalline and amorphous components. The stronger the interaction the higher the depression in the equilibrium melting point. Study of the melting point depression of the crystallizable component in a binary polymer blend can lead to an assessment of the Flory-Huggins interaction parameter χ between the blend components. This parameter results from the condition that the chemical potential of the polymer be identical in the melt and in the pure crystalline state.

One can evaluate χ from the melting points T_m (mixture) and T_m^0 (pure substance) using Nishi-Wang equation³⁸ which was originally based on the Flory-Huggins theory^{39,40}:

$$\frac{1}{T_m} - \frac{1}{T_m^0} = -\frac{RV_2}{\Delta H_f V_1} \left[\frac{\ln \phi_2}{m_2} + \left(\frac{1}{m_2} - \frac{1}{m_1} \right) \phi_1 + \chi \phi_1^2 \right] \quad (3)$$

where the subscript 1 stands for the component, which does not crystallize within the temperature range of interest (TMPC) and 2 represents the crystallizable polymer (PCL). V_1 and V_2 are the molar volumes of the repeating units, ϕ stands for volume fractions, m is the degrees of polymerization, and R is the universal gas constant. ΔH_f signifies the heat of fusion of PCL per monomeric unit.

In the case of polymer/polymer mixtures, where m_1 and m_2 are very large, Eq. (3) reduced to the

following equation:

$$\frac{1}{T_m} - \frac{1}{T_m^0} = -\frac{RV_2}{\Delta H_f V_1} \chi \phi_1^2 \quad (4)$$

The Flory-Huggins interaction parameter χ between the two components can be easily derived from Eq. (4) if one knows the equilibrium melting point depression for a given composition (see the inset-plot of Fig. 2). According to the original ideas of Flory and Huggins, the interaction parameters should be independent of composition. Under these conditions the slope of the straight line passing through the origin of the relationship $1/T_m - 1/T_m^0$ versus ϕ_1^2 should yield χ . The evaluation of the present data according to the above relation (Fig. 3) clearly demonstrates the breakdown of the simplifications. This breakdown may suggest also the remaining of entropy effect. On the basis of the aforementioned data it appears that the equilibrium melting point depression for PCL/TMPC blends result from extrapolating Hoffman-Weeks plots, revealing the presence of interactions between both components. The existence of such interactions is also concluded from the composition dependence of glass-transition temperature.

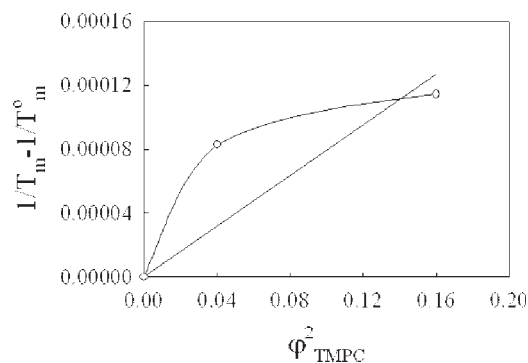


Figure 3 Evaluation of melting point depression for PCL/TMPC blend according to Eq. (4). For mathematical reasons the function must pass through the origin. The straight line shows how the experimental data strongly deviated from Eq. (4).

Isothermal crystallization kinetics

Figure 4 represents a typical isothermal crystallization process for PCL/TMPC = 80/20 blend at different crystallization temperatures. The sample was melted at $T_m = 100^\circ\text{C}$ for 5 min and then rapidly quenched to the crystallization temperature, T_c . Obviously, the crystallization process is strongly influenced by the value of T_c , i.e., the higher the value of T_c the slower the crystallization process. The isothermal crystallization kinetics can be analyzed using Avrami

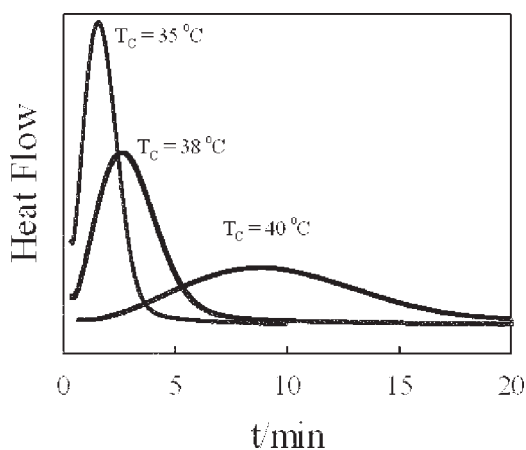


Figure 4 DSC thermograms for the isothermal crystallization of PCL/TMPC = 80/20 blend at different crystallization temperatures T_c . The sample was melted for 5 min at $T_m = 100^\circ\text{C}$ and then rapidly quenched to T_c .

approach.^{25,26} According to this theory the overall crystallization process given by

$$X_t = 1 - \exp(-kt^n) \quad (5)$$

where X_t is the weight fraction crystallized at a time t , k is the rate constant (depending on the crystallization temperature), and n is the Avrami exponent. The rate constant k includes the combined effects of nucleation and growth while n describes the crystal growth geometry and nucleation mechanism.

X_t can be obtained from the DSC signal recorded during the isothermal crystallization process according to the following equation:

$$X_t = \frac{\int_0^t \frac{dH}{dt} dt}{\int_0^\infty \frac{dH}{dt} dt} \quad (6)$$

where the integral in the numerator is the heat generated at time t and that in the denominator is the total heat generated up to the end of crystallization process. The parameters n and k can for instance be obtained from double logarithm plots of $\ln(1 - X_t)$ versus t . An example for such an evaluation is shown in Figure 5. From this figure one can evaluate directly the crystallization half-time $t_{0.5}$ as the time required for $X_t = 0.5$. The value of $t_{0.5}$ or $1/t_{0.5}$ is normally used to describe the overall rate of crystallization process. The value of $t_{0.5}$ as functions of blend composition and crystallization temperature will be discussed later.

Figure 6 shows the Avrami-type plot for PCL/TMPC = 80/20 blend at different T_c . The plot is linear during the initial stage of the crystallization process. A clear deviation from linearity is observed later on. This behavior may be due to the change in

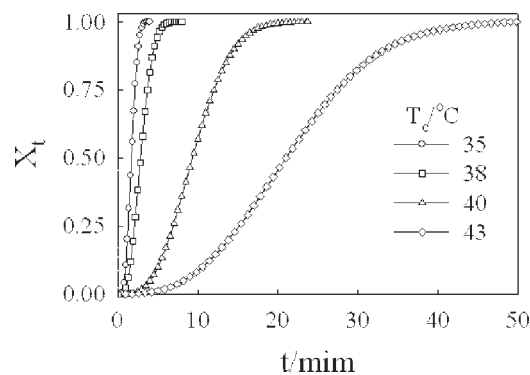


Figure 5 Relative crystallinity X_t as a function of crystallization time t for PCL/TMPC = 80/20 blend at different crystallization temperatures T_c .

the crystallization mechanism from primary crystallization to secondary crystallization. The Avrami equation is based on the assumption that the radial growth of the crystals occurs at a constant velocity, which means that impingement of crystals with one another does not occur. As a result, only the portion of the crystallization isotherms associated with primary crystallization (the first linear part or the crystallization prior to impingement) was used for the determination of the Avrami parameters.⁴¹ The effect of blend composition on the crystallization kinetics can be simply represented in Figures 7 and 8 at constant $T_c = 40^\circ\text{C}$. Obviously the isothermal crystallization kinetics greatly influences by the presence of TMPC, i.e., the process slowed down with increasing the concentration of TMPC in the blend. The values of n and k as functions of composition and temperature are represented in Table I. The values of n in most cases being nonintegral around 3 indicates an athermal nucleation process followed by three-dimensional crystal growth.⁴² However, the nonintegral value of n suggests that n cannot be used to make predictions concerning crystallization mechanisms.

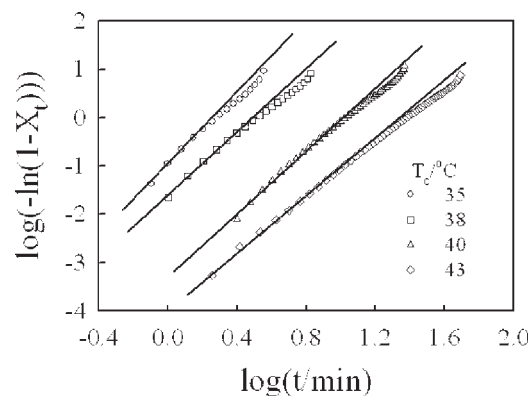


Figure 6 Avrami-type plot for PCL/TMPC = 80/20 blend at different crystallization temperatures T_c .

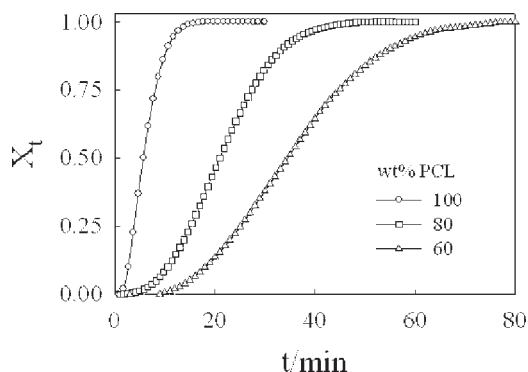


Figure 7 Relative crystallinity X_t as a function of crystallization time t for different PCL/TMPC blend compositions at $T_c = 40^\circ\text{C}$.

The value of n is dependent on the molecular weight. Other reasons for this anomalous value of n could be isothermal thickening, molecular weight fractionation, and so forth.^{41,43-45} The condition employed here (crystallization temperature $T_c = 35\text{--}48^\circ\text{C}$) could favor isothermal thickening. According to this measurement, the rate constant k decreases strongly with increasing the crystallization temperature and concentration of TMPC in the blend. This behavior suggests that the crystallization rate decreases greatly with increasing T_c and concentration of TMPC in the blend. In agreement with current practice, the dimension of k (based on min) is omitted.

The composition dependence of crystallization rate can be well described by the calculation of $t_{0.5}$ at different T_c . Figure 9 represents the relationship between the crystallization temperature (T_c) and $t_{0.5}$ for different blend compositions. For the three samples, the $t_{0.5}$ monotonically increases with the crystallization temperature, as in the common behavior of crystallization rates under cooling. At any crystallization temperature, the $t_{0.5}$ of the blends are longer than the corresponding value for pure PCL. This observation leads to the conclusion that the crystallization of PCL is retarded in the blend because of

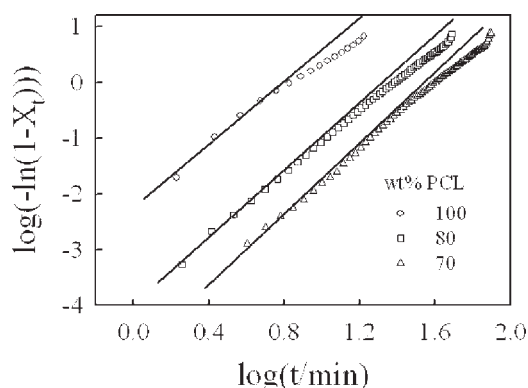


Figure 8 Avrami-type plot for different PCL/TMPC blend compositions at $T_c = 40^\circ\text{C}$.

TABLE I
Kinetic Parameters of Avrami Analyses for Isothermal Crystallization of PCL/TMPC Blends at Different Crystallization Temperatures

wt% PCL	T_c ($^\circ\text{C}$)	n	$\log k$
100	41	2.1	-1.3
	43	2.3	-2.6
	45	3	-3.9
	48	3.3	-7.6
80	35	3.3	-0.95
	38	2.9	-1.5
	40	2.99	-3.1
	43	2.79	-3.819
60	35	2.64	-1.5
	38	2.7	-1.99
	40	2.75	-3.8
	43	2.8	-4.5

the hindrance effect of TMPC for arrangement of the crystallizable chains of PCL. These results are in agreement with Robeson measurements⁴⁶ who studied the effect of polyamide (PA) on the crystallization of poly(ethylene terephthalate) (PET) in PET/PA blend. The isothermal crystallization at 180°C revealed that the time required reaching the maximum crystallization rate varied from 156 s for pure PET to more than 1800 s for the 60/40 PET/PA blend. The difference between the $t_{0.5}$ of the pure PCL and the blends becomes quite clear and large with increasing the crystallization temperature as can be clearly seen in Figure 9. From these results it can be deduced that the overall rate of isothermal crystallization process of PCL is greatly depressed by addition of TMPC.

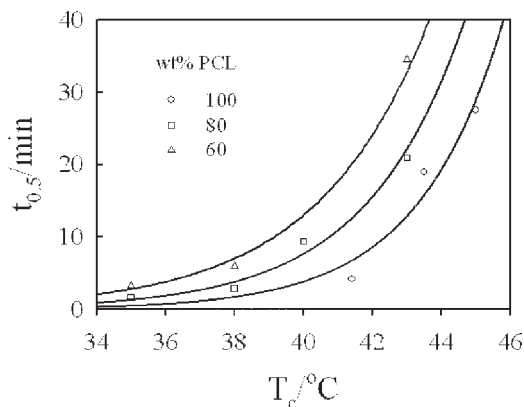


Figure 9 Dependence of the crystallization half-time $t_{0.5}$ on the crystallization temperature T_c for different PCL/TMPC blend compositions.

Spherulite growth rate

It is expected that the morphology and spherulitic growth rate will be strongly influenced by the crystallization temperature and by the presence of a high

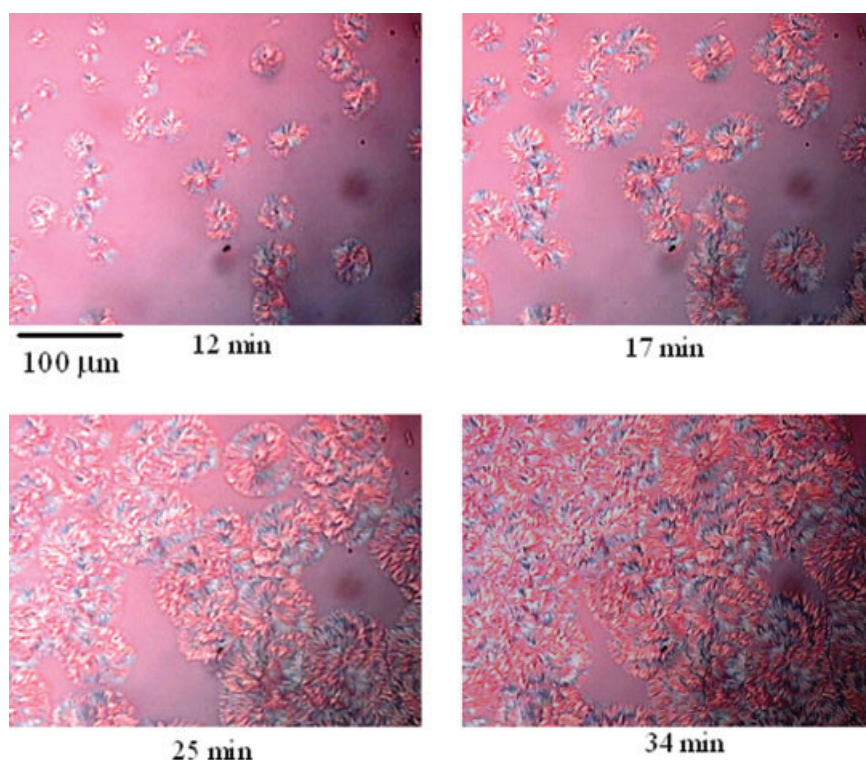


Figure 10 Micrographs documenting the growth of PCL spherulites in PCL/TMPC = 80/20 blend at $T_c = 40^\circ\text{C}$ for different crystallization times. [Color figure can be viewed in the online issue, which is available at www.interscience.wiley.com.]

T_g polymer component in the blend. One point of interest is how the presence of high T_g amorphous component (TMPC) affects the kinetics of spherulitic growth rate of PCL. It is also necessary to understand how the TMPC is accommodated during the crystallization of PCL. In one extreme case the TMPC may be segregated with the uncrystallized melt of PCL to the spherulite growth front which leads in turn to an increase in the concentration of the uncrystallized component at the spherulite front and consequently the growth rate will be decreased at the late stage of the crystallization process. As another extreme, the TMPC may be incorporated entirely into the body of the spherulite in the same concentration as in the melt; in such case there will be no change in the concentration during the crystallization and consequently the spherulitic growth rate will be constant overall the crystallization process. Figure 10 shows an example for the isothermal spherulitic morphology of PCL/TMPC = 80/20 blend at $T_c = 40^\circ\text{C}$ for different time intervals. Figure 11 demonstrates how the radius, R , of the spherulites depends on crystallization time at $T_c = 40^\circ\text{C}$ for different blend compositions. Obviously the growth rate increases linearly with time for all compositions, indicating that the TMPC is incorporated entirely into the body of the spherulite and there is no change in the concentration of the crystallized and noncrystallized component at spherulite front during the

entire time of the crystallization process. Thus the radial diffusion of the rejected noncrystallizable component TMPC is outstripped by the more rapid growth of the crystalline lamellae so that TMPC is trapped between the growing lamellae. It must be mentioned here that the linear behavior of R versus t (Fig. 11) is only valid until near the point where neighboring spherulites impinge. At longer annealing times, the value of R can not be determined accurately. This is not a general behavior for all polymer blends; for example, nonlinear spherulite growth rate and phase change at the spherulite

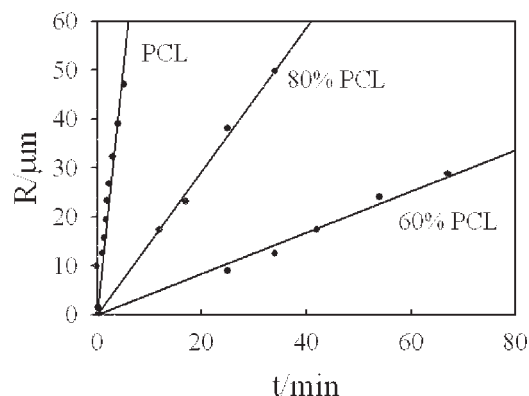


Figure 11 Spherulites radius as a function of crystallization time at $T_c = 40^\circ\text{C}$ for different blend compositions.

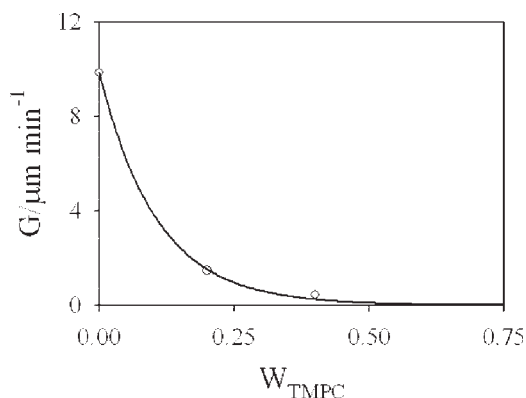


Figure 12 Spherulitic growth rate as a function of weight fraction of TMPC at $T_c = 40^\circ\text{C}$ for different blend compositions.

growth front in isotactic polypropylene/partially hydrogenated oligo(styrene-co-indene) blend was reported by Lee.⁴⁷ The author found nonlinear behavior of the growth rate both at the two-phase region inside the immiscibility loop and at one-phase region just outside the loop.⁴⁷ Previously we detected nonlinear spherulite growth rate for PEO in its mixtures with tetrahydronaphthalene and oligo(ethylene oxide-*b*-dimethylsiloxane) for different concentrations.⁴⁸ This nonlinear behavior was attributed to the segregation and accumulations of the noncrystallizable components to the spherulite growth front.⁴⁸

The slope of the linear relation (Fig. 11) decreases strongly with increasing the concentration of TMPC in the blend which leads to the same conclusion that the crystallization kinetics of PCL retards to a great extent in the presence of TMPC in the blend. Figure 12 reflects this fact very clearly since the spherulitic growth rate ($G = dR/dt$) decreases exponentially with increasing the TMPC concentration in the blend. The difference in the glass-transition temperature of the amorphous constituent and the crystallization temperature is an important factor can strongly influence the spherulitic growth rate of the crystalline component. In the present system, the T_g of TMPC (190°C) is much higher than the crystallization temperatures of PCL ($T_c = 35\text{--}45^\circ\text{C}$). Therefore, both the crystallization kinetics and the spherulitic growth rate decrease strongly with increasing the TMPC concentration in the blend. Another factor which can be considered as a reason for the decreasing of the spherulitic growth rate of PCL in the blend is the dilution of the crystallizable component produced by adding TMPC. It is also related to the change in the chemical potential of the liquid phase due to the specific interaction between the two polymer components. This specific interaction can alter the free energy necessary for the formation of critical nucleus on the crystal surface and the mobility of both

the crystallizable and noncrystallizable components. The influence of mobility is predominant over the influence of the surface free energy related to some experimental parameters such as crystallization temperature, composition of the amorphous component, or the diffusion of amorphous component, thus leading to a decrease of the spherulitic growth rate.

CONCLUSIONS

PCL forms a miscible blend with TMPC over the entire range of composition. Only one common glass-transition temperature was determined; its composition dependence was well described using Gordon-Taylor relation. The isothermal crystallization process of PCL/TMPC blends was investigated at different crystallization temperatures for different blend compositions using DSC technique. The crystallization kinetics was found to be strongly influenced by the crystallization temperature T_c and composition of TMPC in the blend. The isothermal crystallization kinetics of PCL and PCL/TMPC blends could be well described using the Avrami approach. The melting point of PCL was also greatly depressed with increasing the content of TMPC in the blend. From the analysis of the equilibrium melting point depression data, we could obtain information on the Flory-Huggins interaction parameter, χ . The spherulitic radius of PCL in the blends was increased linearly with crystallization time for all different compositions. In addition, the spherulitic growth rate was decreased exponentially with increasing the TMPC concentration in the blend. These experimental facts suggested that the presence of a high T_g amorphous component in the blend retards the crystallization kinetics of PCL to a great extent.

References

- Alfonso, G. C.; Russell, T. P. *Macromolecules* 1986, 19, 1143.
- Conde Brana, M. T.; Iragorri, J. I.; Terselius, B.; Gedde, U. W. *Polymer* 1989, 30, 410.
- Defieuw, G.; Groeninckx, G.; Reinares, H. *Polymer* 1989, 30, 2158.
- Ullmann, W.; Wendorff, J. H. *Compos Sci Technol* 1985, 23, 97.
- Defieuw, G.; Groeninckx, G.; Reinares, H. *Polymer* 1989, 30, 2164.
- Plans, J.; Macknight, W. J.; Karasz, H. E. *Macromolecules* 1984, 17, 810.
- Jo, W. H.; Kim, H. G. *J Polym Sci Part B: Polym Phys* 1991, 29, 1579.
- Kuo, S. W.; Chan, S. C.; Chang, F. C. *Macromolecules* 2003, 36, 6653.
- Schulze, K.; Kressler, J.; Kammer, H. W. *Polymer* 1993, 34, 3704.
- Liu, Z. H.; Marechal, P. H.; Jerome, R. *Polymer* 1996, 37, 5317.
- Janarthanan, V.; Kressler, J.; Karasz, F. E.; Macknight, W. J. *J Polym Sci Part B: Polym Phys* 1993, 31, 1013.
- Inaba, N.; Yamada, T.; Suzuki, S.; Hashimoto, T. *Macromolecules* 1988, 21, 407.

13. Inaba, N.; Sato, K.; Suzuki, S.; Hashimoto, T. *Macromolecules* 1986, 19, 1690.
14. Broz, M. E.; Vander Hart, D. L.; Washburn, N. R. *Biomaterials* 2003, 24, 1690.
15. Wang, Z.; Jiang, B. *Macromolecules* 1997, 30, 6223.
16. Svoboda, P.; Keyzlarova, L.; Saha, P.; Rybnikar, F.; Chiba, T.; Inoue, T. *Polymer* 1999, 40, 459.
17. Kressler, J.; Kammer, H. W. *Polym Bull* 1988, 19, 283.
18. Aoki, Y.; Arendt, O. *J Appl Polym Sci* 2001, 82, 2037.
19. Higashida, N.; Kressler, J.; Inoue, T. *Polymer* 1995, 36, 2761.
20. Chiu, S. C.; Smith, T. G. *J Appl Polym Sci* 1984, 29, 1797.
21. Savoboda, P.; Kressler, J.; Inoue, T. *J Macromol Sci Phys* 1996, 35, 505.
22. Savoboda, P.; Kressler, J.; Chiba, T.; Inoue, T.; Kammer, T. W. *Macromolecules* 1994, 27, 1154.
23. Vanneste, M.; Groeninckx, G. *Polymer* 1995, 36, 4253.
24. Li, Y.; Jungnickel, J. *Polymer* 1993, 34, 9.
25. Avrami, M. *J Chem Phys* 1939, 7, 1103.
26. Avrami, M. *J Chem Phys* 1940, 8, 212.
27. Wunderlich, B. *Macromolecular Physics*; Academic Press: New York, 1976.
28. Herrero, C. H.; Acosta, J. L. *Polym J* 1994, 26, 786.
29. Cebe, P. *Polym Compos* 1988, 9, 271.
30. de Juana, R.; Jáuregui, A.; Calahorra, E.; Cortazar, M. *Polymer* 1996, 37, 3339.
31. Ozawa, T. *Polymer* 1971, 12, 150.
32. Ozawa, T. *Polymer* 1978, 19, 1142.
33. Fox, T. G. *Bull Am Phys Soc* 1956, 2, 123.
34. Gordon, M.; Taylor, J. S. *J Appl Chem* 1952, 2, 493.
35. Mansour, A. A.; Madbouly, S. A. *Polym Int* 1995, 37, 267.
36. Madbouly, S. A. *Polym J* 2002, 34, 515.
37. Hoffman, J. D.; Weeks, J. J. *J Res Natl Bur Stand Sect A* 1962, 66, 14.
38. Nishi, T.; Wang, T. T. *Macromolecules* 1975, 8, 909.
39. Flory, P. J. *Principle of Polymer Chemistry*; Cornell University Press: Ithaca, NY, 1953.
40. Scott, R. L. *J Chem Phys* 1949, 17, 279.
41. Hiemenz, P. C. *Polymer Chemistry*; Marcel Dekker: New York, 1984.
42. Hay, J. N.; Sabir, M.; Steven, R. L. T. *Polymer* 1969, 10, 187.
43. Hong, P. D.; Tsung, W. T.; Hsu, C. F. *Polymer* 2002, 43, 3335.
44. Allen, R. C.; Mandelkern, L. *J Polym Sci Polym Phys Ed* 1982, 20, 1465.
45. Beech, D. R.; Booth, C.; Dodgson, D. V.; Hillier, J. H. *J Polym Sci Part A-2: Polym Phys* 1972, 10, 1555.
46. Robeson, L. *J Appl Polym Sci* 1985, 30, 4081.
47. Lee, C. H. *Polymer* 1998, 39, 5197.
48. Madbouly, S. A.; Wolf, B. A. *J Polym Sci Part B: Polym Phys* 2004, 42, 820.
49. Hay, J. N.; Sabir, M. *Polymer* 1969, 10, 203.